Available online at www.sciencedirect.com

SciVerse ScienceDirect

Ceramics International 38 (2012) 6221–6227

CERAMICS INTERNATIONAL

www.elsevier.com/locate/ceramint

Fabrication of tridoped *p*-ZnO thin film and homojunction by RF magnetron sputtering

L. Balakrishnan, S. Gowrishankar, N. Gopalakrishnan*

Thin Film Laboratory, Department of Physics, National Institute of Technology, Tiruchirappalli 620015, India

Received 26 March 2012; received in revised form 25 April 2012; accepted 26 April 2012
Available online 5 May 2012

Abstract

Tridoping (Al–As–N) into ZnO has been proposed to realize low resistive and stable *p*-ZnO thin film for the fabrication of ZnO homojunction by RF magnetron sputtering. The tridoped films have been grown by sputtering the AlN mixed ZnO ceramic targets (0, 0.5, 1 and 2 mol%) on GaAs substrate at 450 °C. Here, Al and N from the target, and As from the GaAs substrate (back diffusion) takes part into tridoping. The grown films have been characterized by Hall measurement, X-ray diffraction, photoluminescence, time-of-flight secondary ion mass spectroscopy and X-ray photoelectron spectroscopy. It has been found that all the films showed *p*-conductivity except for 2 mol% AlN doped film. The obtained resistivity ($8.6 \times 10^{-2}\,\Omega\,cm$) and hole concentration ($4.7 \times 10^{20}\,cm^{-3}$) for the best tridoped film (1 mol% AlN) is much better than that of monodoped and codoped ZnO films. It has been predicted that $[(As_{Zn} - 2V_{Zn}) + N_O]$ acceptor complex is responsible for the *p*-conduction. The homojunction fabricated using the best tridoped ZnO film showed typical rectifying characteristics of a diode. The junction parameters have been determined for the fabricated homojunction by Norde's and Cheung's method.

Keywords: ZnO; Tridoping; *p*-conductivity; Homojunction

1. Introduction

Zinc oxide (ZnO) or zinc white had long been used as a major white pigment in decorative paints, ointments and as an industrial chemical. However, the intense research on ZnO started gradually around 1930s with the investigation of structural and physical properties [1]. In the past two decades, ZnO has proven to show a variety of multi-functional properties viz., transparent conducting electrodes in solar cells, piezoelectric material in surface acoustic wave devices and single crystalline substrate for GaN thin film growth [2,3]. In recent years, ZnO has been considered as one of the most promising material for optoelectronic applications (UV LEDs and LDs) because of its splendor properties such as high excitonic binding energy, high optical gain, high radiation and temperature stability [4]. In order to develop the ZnO based optoelectronic devices, the first step is the fabrication of high quality *n*- and *p*- type ZnO thin films. It is easy to grow good quality *n*-type ZnO with resistivity 1–2 order of magnitude higher than metals because of its intrinsic non-stoichiometric growth [5]. Hence, *p*-conductivity can be realized only by doping group-I elements on Zn site or group-V elements on O site. All possible dopants and doping methods such as monodoping, codoping and cluster doping have been tried to realize low resistive *p*-ZnO but only few of them are succeeded despite the stability of the *p*-conduction remains to be answered [6–9].

In this article, we made an attempt on tridoping using AlN mixed ZnO ceramic targets and GaAs substrate to realize low resistive and stable *p*-ZnO. In our tridoping, we have used GaAs substrate as the source of supplying Arsenic atoms by taking the advantage of As back diffusion from the substrate. In tridoping, N and As substitutes on O and Zn sites, respectively which leads to the formation of

*Corresponding author. Tel.: +91 431 2503607; fax: +91 431 2500133.
E-mail address: ngk@nitt.edu (N. Gopalakrishnan).

0272-8842/$36.00
http://dx.doi.org/10.1016/j.ceramint.2012.04.075

shallow acceptor complexes (N_O and $As_{Zn}-2V_{Zn}$) [8–10]. Further, Al increases the solubility of acceptors due to the formation of acceptor–donor–acceptor complex [5].

In tridoping, N substitutes on O site and forms a shallow acceptor (N_O) as both has similar atomic radius. However, as there is large radii misfit between As and O, As substitutes on Zn site (As_{Zn}) and combines with two Zn vacancies, forms stable ($As_{Zn}-2V_{Zn}$) shallow acceptor complex [10]. The formation this complex has been explained as follows,

$$(As_{Zn}-V_{Zn})^{+}+V_{Zn}^{2-}\rightarrow(As_{Zn}-2V_{Zn})^{-}$$

The acceptor ionization energy for this complex is very low (~200 meV) compared to As_O (~930 meV). Hence, the probability of inducing *p*-conduction by As_O is very low in As doped ZnO.

Here, the effect of AlN concentration on *p*-conductivity of tridoped ZnO films has been investigated in detail. The homojunction has also been fabricated using best tridoped *p*-ZnO film and 2% Al doped *n*-ZnO film. The *I–V* measurement has been made for the fabricated homojunction and hence the junction parameters determined.

2. Experimental

Al–As–N tridoping have been achieved by sputtering the AlN mixed ZnO ceramic target on semi-insulating GaAs substrates. AlN mixed ZnO targets of different concentration (0, 0.5, 1 and 2 mol%) for sputtering have been prepared by conventional solid-state reaction route. AlN powder of required amount has been mixed uniformly with ZnO in planetary ball milling for 10 h. The mixed powder has been made into a circular disk (55 mm dia.) using pelletizer (200 psi pressure) followed by annealing (950 °C) for 6 h to densify the target. The GaAs substrate cleaned in boiling acetone, ethanol and rinsed in distilled water for 3–5 times has been loaded into the chamber. Thus prepared target and substrate have been fixed at a distance of separation, 5 cm. Initially, the chamber has been evacuated to a base pressure, 8×10^{-6} mbar and then Ar (sputtering gas) and O_2 (reactive gas) have been flown into the chamber at a total pressure of 0.02 mbar. The sputtering has been carried out for 30 min at 100 W power and substrate temperature, 450 °C. The optimized substrate temperature of 450 °C has been used because As atoms start diffuse into ZnO (back diffusion) when the temperature is greater than 400 °C. Further, if the temperature is greater than 500 °C, the vapor pressure of Ga starts to rise which leads to the diffusion of Ga atoms [11]. The grown tridoped films with different AlN concentrations have been characterized by Hall measurement, X-ray diffraction (XRD), time-of-flight secondary ion mass spectroscopy (ToF-SIMS), X-ray photoelectron spectroscopy (XPS), room temperature and low temperature photoluminescence (PL). Further, the best tridoped *p*-ZnO film (1 mol% AlN doped ZnO:As) has been used to fabricate the homojunction. The junction parameters have been determined for the fabricated homojunction.

3. Results and discussion

3.1. Electrical properties

The electrical properties of the films have been studied using Van der Pauw Hall effect measurement system at room temperature. Table 1 shows the electrical properties of the tridoped ZnO films with respect to AlN doping concentration. It is seen that the monodoped film (AlN = 0%) showed *p*-conductivity with the hole concentration, $\sim10^{15}$ cm^{-3} due to the diffusion of As atoms into ZnO. Here, the As sits on Zn site and thereby forms ($As_{Zn}-2V_{Zn}$) complexes which gives rise to *p*-conductivity [10]. Further, the hole concentration increases with the increase of AlN concentration (till 1 mol%) due to the incorporation of both N and As acceptors into ZnO. In tridoping, As sits on Zn site while N sits on O site and forms ($As_{Zn}-2V_{Zn}$) and N_O acceptor complexes, respectively which causes *p*-conductivity. However, for 2 mol% AlN doped ZnO, the conductivity changes from *p*- to *n*-type. This might be due to the incorporation of more Al, N and As atoms which lead to the formation of donor complexes such as Al_{Zn}, N_i, N_2, As_{Zn}, $As_{Zn}-V_{Zn}$, etc. [12]. Among the *p*-ZnO films, 1 mol% AlN doped film showed high hole concentration $\sim10^{20}$ cm^{-3} due to the optimum incorporation of Al, As and N atoms. Hence, 1 mol% AlN doped ZnO:As film has been considered as a best tridoped film. Further, the conductivity and hole concentration remains approximately same even after six months. It reveals the stability of tridoped *p*-ZnO thin films. Similarly, in order to check the reproducibility of our films, the best tridoped *p*-ZnO film has been grown couple of times before fabricating the junction. It showed *p*-conductivity with almost equal hole concentration and resistivity.

Table 1
Hall measurements of monodoped and tridoped ZnO films with different AlN doping concentration.

AlN concentration (mol%)	Carrier type	Carrier concentration (cm^{-3})	Resistivity (Ω cm)	Mobility (cm^2/Vs)
0	*p*	9.33×10^{15}	18.67	35.82
0.5	*p*	5.03×10^{19}	3.86×10^{-2}	3.602
1	*p*	4.72×10^{20}	8.63×10^{-2}	0.536
2	*n*	1.17×10^{20}	8.35×10^{-2}	0.867

3.2. Structural properties

3.2.1. XRD analysis

The crystallinity of the films has been studied using XRD. Fig. 1 shows the XRD pattern of Al–As–N tridoped ZnO films of different AlN doping concentration. It is seen

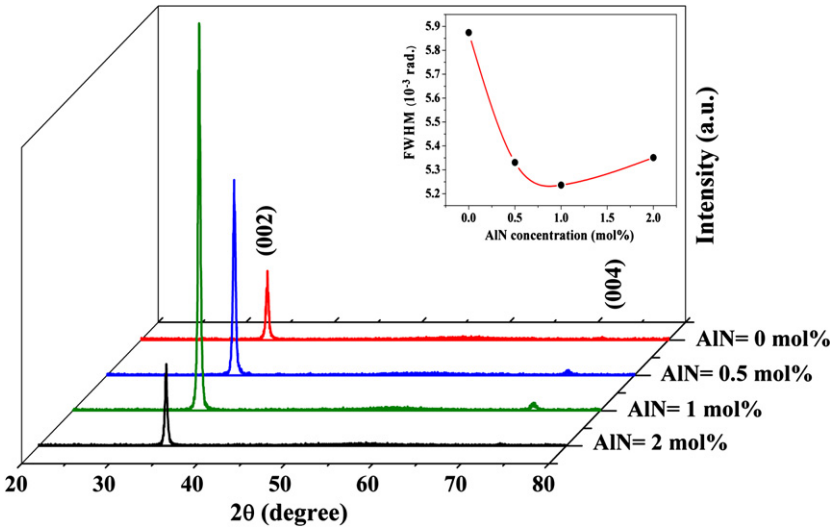

Fig. 1. XRD pattern of Al–As–N tridoped ZnO films of different AlN doping concentration. Inset: Variation of grain size with respect to AlN concentration.

that all the films are preferentially oriented along (002) plane (*c*-axis) with hexagonal wurtzite structure, and free from the formation of secondary phases. A weak (004) plane (*a*-axis) diffraction has also been observed. The inset shows the variation of full-width at half maximum (FWHM) of (002) plane with respect to AlN concentration. From the inset, it is understood that the crystallinity increases with the increase of AlN concentration due to the improvement of stoichiometry and solubility by the incorporation of N and Al ions on O and Zn sites, respectively. For 2 mol% AlN doped ZnO, the degradation in crystallinity might be due to the non-stoichiometry. The non-stoichiometry arises due to the more incorporation of Al and N atoms above the solubility limit that leads to the formation of Al, N and As related defects which in turn degrades the crystallinity [12]. These observations have been well supported by our Hall effect measurement results.

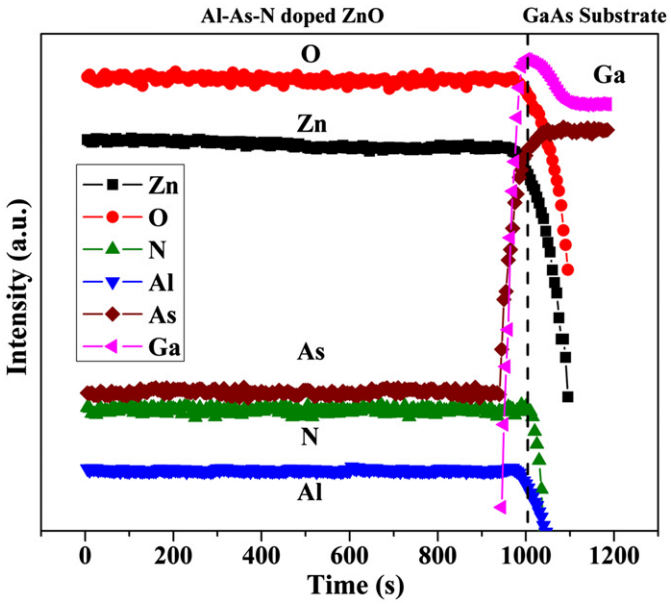

Fig. 2. ToF-SIMS depth profile of 1 mol% AlN doped ZnO:As.

3.3. Elemental properties

3.3.1. ToF-SIMS analysis

In order to confirm the diffusion of As atoms into ZnO and homogeneity of the dopants in the film ToF-SIMS analysis has been performed. Fig. 2 shows the depth profile of 1 mol% AlN doped ZnO film grown on GaAs substrate. It evident that As atoms alone diffused (back diffused) into the film. Further, the flat profile of Al and N indicates that the dopants are uniformly doped into the film. Moreover, it shows that the concentration of O atoms is greater than Zn atoms inspite of natural ZnO which is non-stoichiometry in the form of oxygen deficiency (i.e. Zn rich) [10]. The higher concentration of O atoms compared to Zn atoms reveal the presence of Zn vacancies (i.e. V_{Zn}) in the film. It confirms the presence of V_{Zn} due to the incorporation of As atoms into ZnO and indirectly supports the formation of $(As_{Zn}-2V_{Zn})$ complex. It should be again noted that the concentration of acceptors (As and N) are more than donors (Al) which well supports the *p*-conductivity of the films.

3.3.2. XPS analysis

In order to understand the *p*-type formation mechanism and chemical bonding states of the elements, XPS analysis has been performed. Fig. 3 shows the core level XPS spectra of the constituents in the 1 mol% AlN doped ZnO:As film. In Zn-2p core level spectrum (Fig. 3(a)), the peak at the binding energy, 1021.3 and 1044.6 eV corresponds to $Zn-2p_{3/2}$ and $Zn-2p_{1/2}$, respectively confirms that most of the zinc atoms exist in Zn–O bond [13]. In

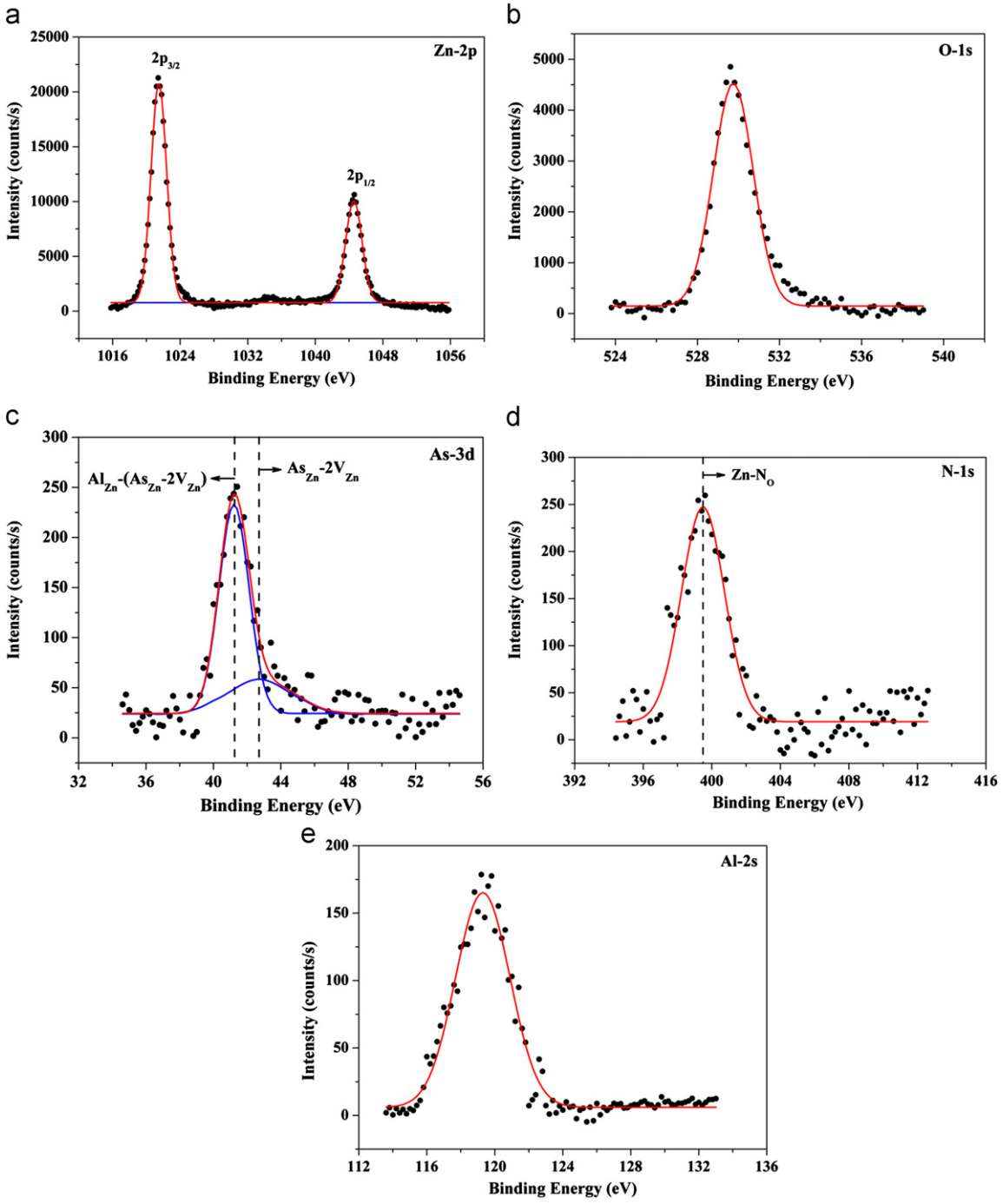

Fig. 3. Core level XPS spectra of (a) Zn-2p, (b) O-1s, (c) As-3d, (d) N-1s and (e) Al-2s for 1 mol% AlN doped ZnO:As film.

O-1s core level spectrum (Fig. 3(b)), the peak at the binding energy of 529.6 eV implies that most of the O atoms are in Zn–O coordination [14]. The smaller value of binding energy for Zn-2p and O-1s compared to Zn and O in bulk ZnO implies that majority of Zn and O ions are in Zn deficient ZnO matrix [14,15]. In order to clearly illustrate the *p*-type formation mechanism, the core level XPS spectra of donor and acceptor dopants have also been performed. In As-3d core level spectrum (Fig. 3(c)), the broad peak centered at the binding energy of 41 eV speculate that the As-atoms exist in the state of $(As_{Zn}-2V_{Zn})$ complex. In order to further analyze the enhanced *p*-conductivity, the spectrum has been deconvoluted into two gaussion curves centered at 42.6 and 41 eV. The smaller peak at the binding energy of 42.6 eV implies that low concentration of $(As_{Zn}-2V_{Zn})$ complexes are in the isolated state [16]. Further, the strong peak at the binding energy of 41 eV implies that most of the $(As_{Zn}-2V_{Zn})$ acceptors are in columbic interaction with Al_{Zn} donor due to the formation of acceptor–donor–acceptor complex as

in codoping [17,18]. This gives rise to the enhanced *p*-conductivity due to the more incorporation of As atoms into the film. In N-1s core level spectrum (Fig. 3(d)), the sharp peak at the binding energy of 399.5 eV confirms the Zn–N bond (i.e. N_O) unlike Al–N bond as in AlN codoping which also indirectly confirms that Al atoms are in close interaction with ($As_{Zn}-2V_{Zn}$) acceptors [19]. Similarly, in Al-2s core level spectrum (Fig. 3(e)), the peak at the binding energy of 119.3 eV confirms the Al_{Zn} formation and Al–As close interaction [20]. From the XPS analysis, it has been concluded that the observed strong *p*-conductivity is due the formation of $[(As_{Zn}-2V_{Zn})+N_O]$ acceptor complexes. Based on these analysis and theoretical predictions [10], the *p*-type formation mechanism can be explained by the following equation,

$$(As_{Zn}-2V_{Zn})^{-}+Al_{Zn}^{+}+(As_{Zn}-2V_{Zn})^{-}+N_O^{-} \rightarrow (Al_{Zn}+2As_{Zn}-4V_{Zn}+N_O)^{2-}$$

3.4. Optical properties

3.4.1. Room temperature PL analysis

Fig. 4 shows the PL spectra of AlN doped ZnO:As thin films grown on GaAs substrate with respect to AlN doping concentration. It is seen that all the films showed strong violet luminescence (VB) at around 3 eV and deep level emissions such as blue band (BB) at around 2.8 eV, green band (GB)~2.54 eV and yellow band (YB) ~2.4 eV. It has been reported that the violet luminescence in ZnO is due to the radiative transition between conduction band and V_{Zn} acceptor level [21]. From the spectra, it is seen that the intensity of violet luminescence increases with increase of Al–N doping concentration. This is due to the more incorporation of As atoms caused by the increase in solubility. However, for 2 mol% AlN doped ZnO:As film, the decrease in intensity is due to the more incorporation

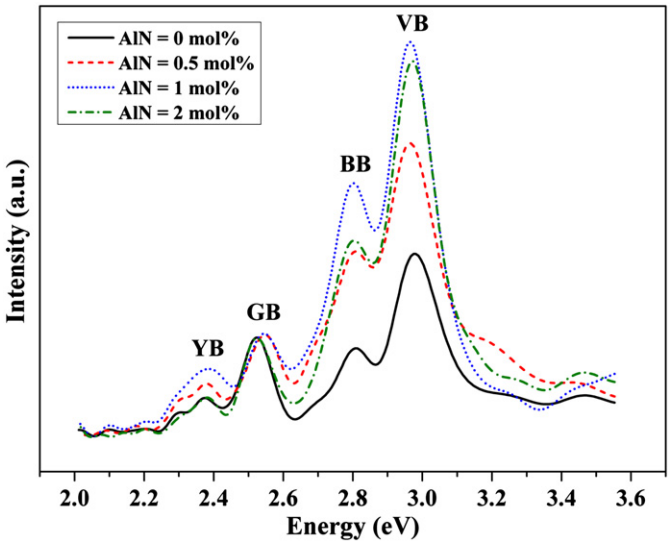

Fig. 4. Room temperature (300 K) PL spectra of AlN doped ZnO:As thin films of different AlN doping concentration.

of Al, N and As ions which might be leads to the formation of more donors complexes such as $As_{Zn}-V_{Zn}$, As_{Zn}, Al_{Zn}, N_2, etc [22,23]. This has been well supported by our Hall effect measurement and XRD results. Further, the defect level emission such as BB, GB and YB are due to the lattice distortion induced by inclusion of large radii atoms [24], radial recombination of photogenerated hole with an electron [25] and free electron to deep acceptor levels [26], respectively.

3.4.2. Low temperature PL analysis

In order to further confirm the *p*-conductivity again, low temperature (10 K) PL measurement has been performed for the best tridoped ZnO film. Fig. 5 shows the low temperature PL spectra of 1 mol% AlN doped ZnO:As film. The dominant emission peaks located at around 2.9 and 3.12 eV are ascribed to the emission related to V_{Zn} and N acceptor levels which has been indicated as $A^{O}_{V_{Zn}}$ and DA_NP, respectively [27–29]. The peaks located at 3.23 and 3.27 eV are attributed to the donor-acceptor-pair (DAP) emission and neutral-acceptor-bound exciton recombination ($A^{O}X$), respectively which confirms the presence of acceptors in the film [30,31]. Further, the dominant $A^{O}_{V_{Zn}}$ peak intensity compared to DA_NP implies that V_{Zn} related complex i.e. $(As_{Zn}-2V_{Zn})$ involves more compared to N_O for *p*-conduction in tridoped ZnO films. This has been also well supported by our ToF-SIMS analysis.

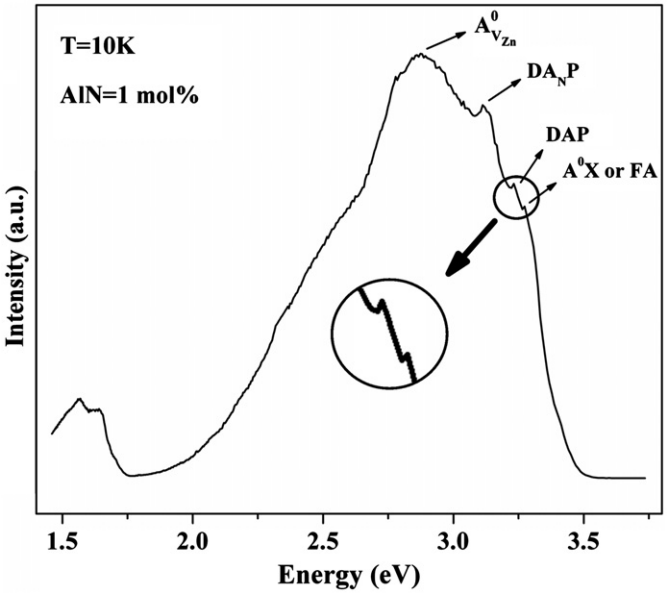

Fig. 5. Low temperature (10 K) PL spectra of 1 mol% AlN doped ZnO:As film.

3.5. Fabrication of ZnO homojunction

ZnO homojunction has been fabricated using the best tridoped ZnO film. The homojunction has been fabricated by growing 2 at% Al doped ZnO film (*n*-ZnO) on best tridoped ZnO film (*p*-ZnO). Al electrodes for the electrical

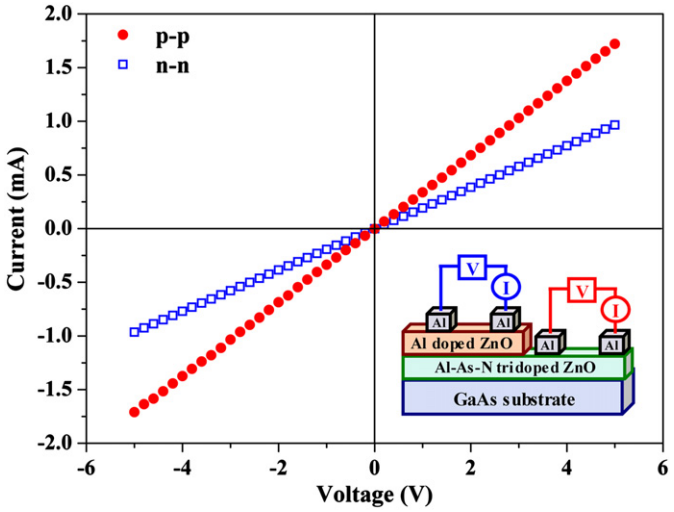

Fig. 6. Ohmic characteristics of Al contact to *p*- and *n*-ZnO film.

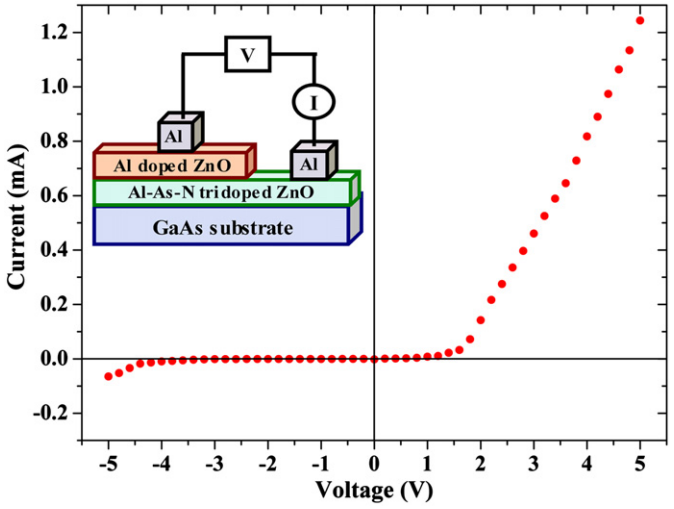

Fig. 7. *I–V* characteristics of the *p*-ZnO:(Al, As, N)/*n*-ZnO:Al homojunction.

contacts have been deposited on both *p*- and *n*-type ZnO films by thermal evaporation. Fig. 6 shows the current–voltage (*I–V*) characteristics of the contacts deposited on both films. The linear *I–V* dependents confirm the ohmic behavior of the contacts.

Fig. 7 shows the *I–V* characteristics of the fabricated ZnO homojunction. It shows typical rectifying behavior of a diode which acknowledges the success of our tridoping method to realize *p*-ZnO. Further, the diode parameters such as ideality factor, series resistance and barrier height have been determined using Norde's and Cheung's methods [32,33]. The ideality factor, series resistance and barrier height values have been found as 6.9, 2.4 kΩ and 0.84 eV, respectively.

4. Conclusion

A tridoping approach has been proposed for the fabrication of low resistive and stable *p*-ZnO thin film by RF magnetron sputtering. The tridoping (Al–As–N) has been done by sputtering the AlN mixed ZnO ceramic targets (0, 0.5, 1 and 2 mol%) on GaAs substrate. The advantage of As back diffusion from the GaAs substrate has been used as As source. The grown tridoped ZnO films of different AlN concentration have been characterized by Hall effect measurement, XRD and PL. Hall measurements showed that all the films are *p*-conductivity except 2 mol% AlN doped film. It has been found that the hole concentration increases with increase of AlN doping concentration till 1 mol% AlN and the conductivity changes to *n*-type with further increase of AlN concentration. Among the *p*-ZnO films, 1 mol% AlN doped ZnO:As shows high hole concentration due to the best tridoping effect. The Hall measurement results have been well supported by XRD and PL analysis. The presence of dopants in the film has been confirmed by ToF-SIMS. The chemical bonding states of the elements in the film has been determined by XPS and it confirmed that $[(As_{Zn}-2V_{Zn})+N_O]$ acceptor complex is responsible for the observed *p*-conductivity in tridoped ZnO films. The *p*-conductivity of the films has been also confirmed by low temperature PL measurement. The fabricated homojunction using best tridoped film shows good rectifying behavior which confirms the success of the tridoping approach.

Acknowledgment

The authors are thankful to Technical Education Quality Improvement Program (TEQIP), Government of India for providing the instrument facilities. The authors are also thankful to Dr. S.R. Barman, UGC-DAE Consortium for Scientific Research, Indore 452001, India for extending the XPS facility.

References

[1] H. Pauling, The sizes of ions and the structure of ionic crystals, Journal of the American Chemical Society 49 (1927) 765–790.
[2] A.E. Delahoy, M. Cherny, Deposition schemes for low cost transparent conductors for photovoltaics, Materials Research Society Symposium Proceedings 426 (1996) 467–477.
[3] K.L. Chopra, S. Major, D.K. Pandya, Transparent conductors—A status review, Thin Solid Films 102 (1983) 1–46.
[4] C. Klingshirn, The luminescence of ZnO under high one- and two-quantum excitation, Physica Status Solidi B: Basic Solid State Physics 71 (1975) 547–556.
[5] T. Yamamoto, H.K. Yoshida, Physics and control of valence states in ZnO by codoping method, Physica B:Condensed Matter 302–303 (2001) 155–162.
[6] J.G. Lu, Y.Z. Zhang, Z.Z. Ye, L.P. Zhu, L. Wang, B.H. Zhao, Q.L. Liang, Low-resistivity, stable p-type ZnO thin films realized using a Li–N dual-acceptor doping method, Applied Physics Letters 88 (2006) 222114.
[7] Y.Z. Zhang, J.G. Lu, Z.Z. Ye, H.P. He, L.P. Zhu, B.H. Zhao, L. Wang, Effects of growth temperature on Li–N dual-doped p-type ZnO thin films prepared by pulsed laser deposition, Applied Surface Science 254 (2008) 1993–1996.
[8] M. Kumar, T.-H. Kim, S.-S. Kim, B.-T. Lee, Growth of epitaxial p-type ZnO thin films by codoping of Ga and N, Applied Physics Letters 89 (2006) 112103.

[9] H. Kim, A. Cepler, M.S. Osofsky, R.C.Y. Auyeung, A. Pique, Fabrication of Zr–N codoped p-type ZnO thin films by pulsed laser deposition, Applied Physics Letters 90 (2007) 203508.
[10] S. Limpijumnong, S.B. Zhang, S.H. Wei, C.H. Park, Doping by large-size-mismatched impurities: the microscopic origin of arsenic- or antimony-doped p-type zinc oxide, Physical Review Letters 92 (2004) 155504.
[11] K.S. Huh, D.K. Hwang, K.H. Bang, M.K. Hong, D.H. Lee, J.M. Myong, M.S. Oh, W.K. Choi, Effects of As Doping on Properties of ZnO Films, Materials Research Society Symposium Proceedings 692 (2002) 649–654.
[12] E.C. Lee, Y.S. Kim, Y.G. Jin, K.J. Chang, Compensation mechanism for N acceptors in ZnO, Physical Review B 64 (2001) 085120.
[13] M. Sano, T. Adaniya, T. Fujitani, J. Nakamura, Oxidation of a Zn-deposited Cu(1 1 1) surface studied by XPS and STM, Surface Science 514 (2002) 261–266.
[14] M. Chen, X. Wang, Y.H. Yu, Z.L. Pei, X.D. Bai, C. Sun, R.F. Huang, L.S. Wen, X-ray photoelectron spectroscopy and auger electron spectroscopy studies of Al-doped ZnO films, Applied Surface Science 158 (2000) 134–140.
[15] S. Major, S. Kumar, M. Bhatnagar, K.L. Chopra, Effect of hydrogen plasma treatment on transparent conducting oxides, Applied Physics Letters 49 (1986) 394.
[16] H.S. Kang, G.H. Kim, D.L. Kim, H.W. Chang, B.D. Ahn, S.Y. Lee, Investigation on the p-type formation mechanism of arsenic doped p-type ZnO thin film, Applied Physics Letters 89 (2006) 181103.
[17] J.A. Taylor, An XPS study of the oxidation of AlAs thin films grown by MBE, Journal of Vacuum Science and Technology 20 (1982) 751.
[18] E. Rita, Ph.D. Thesis, Departamento de Física, Universidade de Lisboa, Portugal, 2008.
[19] M. Joseph, H. Tabata, H. Saeki, K. Ueda, T. Kawai, Fabrication of the low-resistive p-type ZnO by codoping method, Physica B:Condensed Matter 302–303 (2001) 140–148.
[20] B. Vincent Crist, Hand Book of Monochromatic XPS Spectra, vol. 2, XPS International, LLC, United States of America, 2005.
[21] B.J. Jin, S. Im, S.Y. Lee, Violet and UV luminescence emitted from ZnO thin films grown on sapphire by pulsed laser deposition, Thin Solid Films 366 (2000) 107–110.
[22] J. Wang, V. Sallet, F. Jomard, A.M.B. Do Rego, E. Elamurugu, R. Martins, E. Fortunato, Influence of the reactive N_2 gas flow on the properties of rf-sputtered ZnO thin films, Thin Solid Films 515 (2007) 8780–8784.
[23] J.C. Fan, Z. Xie, Effects of substrate temperature on structural, electrical and optical properties of As-doped ZnO films, Materials Science and Engineering B 150 (2008) 61–65.
[24] Y.R. Ryu, T.S. Lee, J.A. Lubguban, H.W. White, Y.S. Park, C.J. Youn, ZnO devices: Photodiodes and p-type field-effect transistors, Applied Physics Letters 87 (2005) 153504.
[25] K. Vanheusden, W.L. Warren, C.H. Seager, D.R. Tallant, J.A. Voigt, B.E. Gnade, Mechanisms behind green photoluminescence in ZnO phosphor powders, Journal of Applied Physics 79 (1996) 7983.
[26] D.H. Fan, Z.Y. Ning, M.F. Jiang, Characteristics and luminescence of Ge doped ZnO films prepared by alternate radio frequency magnetron sputtering, Applied Surface Science 245 (2005) 414–419.
[27] F.X. Xiu, Z. Yang, L.J. Mandalapu, D.T. Zhao, J.L. Liua, Photoluminescence study of Sb-doped p-type ZnO films by molecular-beam epitaxy, Applied Physics Letters 87 (2005) 252102.
[28] D.J. Rogers, T.F. Hosseini, T. Monteiro, M. Soares, A. Neves, M. Carmo, S. Pereira, M.R. Correia, A. Lusson, E. Alves, N.P. Barradas, J.K. Morrod, K.A. Prior, P. Kung, A. Yasan, M. Razeghi, Investigations of p-type signal for ZnO thin films grown on (100) GaAs substrates by pulsed laser deposition, Physica Status Solidi C: Current Topics in Solid State Physics 3 (2006) 1038–1041.
[29] H. Tang, Z. Ye, H. He, Comparative photoluminescence study on p-type and n-type ZnO films codoped by nitrogen and aluminium, Optical Materials 30 (2008) 1422–1426.
[30] E. Przezdziecka, E. Kaminska, I. Pasternak, A. Piotrowska, J. Kossut, Photoluminescence study of p-type ZnO:Sb prepared by thermal oxidation of the Zn-Sb starting material, Physical Review B 76 (2007) 193303.
[31] S.S. Lin, J.G. Lu, Z.Z. Ye, H.P. He, X.Q. Gu, L.X. Chen, J.Y. Huang, B.H. Zhao, p-type behavior in Na-doped ZnO films and ZnO homojunction light-emitting diodes, Solid State Communications 148 (2008) 25–28.
[32] H. Norde, A modified forward I-V plot for Schottky diodes with high series resistance, Journal of Applied Physics 50 (1979) 5052.
[33] S.K. Cheung, N.W. Cheung, Extraction of Schottky diode parameters from forward current-voltage characteristics, Applied Physics Letters 49 (1986) 85.